

Continuous phase transitions between fractional quantum Hall states and symmetry-protected topological states

Ying-Hai Wu

*School of Physics and Wuhan National High Magnetic Field Center,
Huazhong University of Science and Technology, Wuhan 430074, China*

Hong-Hao Tu

Institut für Theoretische Physik, Technische Universität Dresden, 01062 Dresden, Germany

Meng Cheng

Department of Physics, Yale University, New Haven, Connecticut 06511-8499, USA

We study quantum phase transitions in Bose-Fermi mixtures driven by interspecies interaction in the quantum Hall regime. In the absence of such an interaction, the bosons and fermions form their respective fractional quantum Hall (FQH) states at certain filling factors. A symmetry-protected topological (SPT) state is identified as the ground state for strong interspecies interaction. The phase transitions between them are proposed to be described by Chern-Simons-Higgs field theories. For a simple microscopic Hamiltonian, we present numerical evidence for the existence of the SPT state and a continuous transition to the FQH state. It is also found that the entanglement entropy between the bosons and fermions exhibits scaling behavior in the vicinity of this transition.

Introduction — The collective behavior of a large number of microscopic objects is a fascinating topic. In quantum condensed matter physics, one central task is to elucidate the possible phases and transitions between them for a given many-body system. A large class of phases and transitions is characterized by spontaneous breaking of global symmetries, described by the Landau-Ginzburg theory. However, quantum phases of matter beyond the symmetry-breaking framework have also been discovered, a notable example being topological states in quantum Hall systems [1–3]. In the simplest cases, the integer quantum Hall (IQH) states can be understood as free electrons filling Landau levels. On the contrary, fractional quantum Hall (FQH) states only appear in strongly correlated systems. Fractionalized elementary excitations, multiple ground states on high-genus manifolds, and long-range quantum entanglement are their hallmarks. The fact that quantum Hall states do not fit into the symmetry paradigm prompts the questions: what are the possible quantum phase transitions that involve quantum Hall states and how to characterize them? Previous works have investigated transitions between different IQH states [4–7], between different FQH states [8–11], and between certain IQH or FQH states and non-topological states [12–22].

The discovery of topological insulators greatly expanded the realm of topological phases [23, 24]. One crucial insight of this adventure is that time-reversal and charge conservation symmetries should be preserved for these states to be nontrivial [25–28]. Further progress along this line leads to the concept of symmetry-protected topological (SPT) states [29–35]. This generalization incorporates strongly correlated states of spins, bosons, and fermions that exhibit nontrivial symmetry-protected edge physics but do not possess fractionalized

excitations in the bulk. Quantum phase transitions from SPT states to trivial states or symmetry-breaking states have been studied [36–52].

In this work, we study a new class of topological phase transitions between SPT and FQH states in Bose-Fermi mixtures in the quantum Hall regime. We show that a SPT state can be realized for Bose-Fermi mixtures under suitable conditions, and it goes through a continuous transition to two decoupled FQH states as the interspecies interaction decreases. Experimentally, while fermionic quantum Hall states are routinely realized in solid state systems, bosonic ones are more challenging to realize [53–61]. For cold atoms, Bose-Fermi mixtures have been extensively explored [62–65]. In solid state systems, electrons and holes may combine to form bosonic excitons. Electrons and excitons may coexist and form correlated Bose-Fermi mixtures in transition metal dichalcogenides [66, 67]. In addition, a recent work has reported evidence for the bosonic Laughlin state of excitons [68]. FQH states of excitons have also been proposed for moiré systems [69, 70]. This progress provides strong motivations for our investigations of FQH states and phase transitions in Bose-Fermi mixtures.

Wave functions and field theories for the SPT and FQH states — We start with trial wave functions for the SPT and FQH states in Landau levels, which will shine light on the nature of the transition. The letter b (f) is used as subscripts or superscripts to represent bosons (fermions). For instance, the numbers of particles are denoted as N_b and N_f . As illustrated in Fig. 1, the bosons and fermions are subjected to two independent magnetic fields with total fluxes M_b and M_f , so their filling factors are $\nu_b = \frac{N_b}{M_b}$ and $\nu_f = \frac{N_f}{M_f}$. A positive direction for the magnetic fields is chosen so each filling factor has its

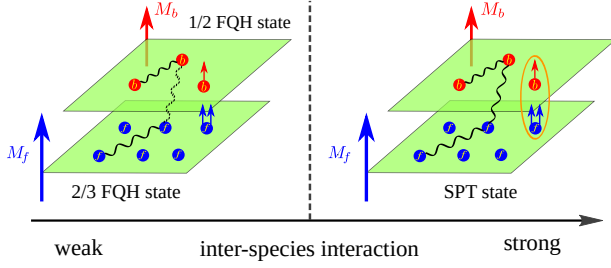


FIG. 1. Illustration of the quantum phase transition in Bose-Fermi mixtures. The solid (dashed) wiggly lines represent strong (weak) interactions between the particles. If there is no interspecies interaction, two independent FQH states are formed in which the particles are transformed to composite fermions (indicated by the small arrows). As the interspecies interaction strength grows, the two types of composite fermions eventually become strongly correlated to form the SPT state.

sign. The IQH state with $\nu = n > 0$ is denoted as Φ_n and that with $\nu = -n$ is Φ_n^* . Throughout this work, we assume that the bosons/fermions carry a $U(1)$ charge e_b/e_f . While in solid state systems one usually takes $e_f = 1$ and e_b an even integer (e.g. $e_b = 2$ for Cooper pairs), this is not necessarily the case for cold atoms because they are actually charge neutral. Analogs of Hall conductance can be studied and the specific probing method determines the “effective” charge of atoms [59].

In terms of the complex coordinates z_j, z_k, \dots on the plane, the SPT state is described by

$$\Psi_{\text{SPT}} \sim \left[\Phi_1^*(\{z_j^b\}) \Phi_1^*(\{z_j^f\}) \right] \prod_j^{N_b} \prod_k^{N_f} (z_j^b - z_k^f) \times \prod_{j < k}^{N_b} (z_j^b - z_k^b) \prod_{j < k}^{N_f} (z_j^f - z_k^f)^2. \quad (1)$$

It can be interpreted using the flux attachment process that maps strongly correlated particles to noninteracting composite fermions [71]: The bosons (fermions) are converted to composite fermions by the Jastrow factor $\prod_{j < k}^{N_b} (z_j^b - z_k^b) \left[\prod_{j < k}^{N_f} (z_j^f - z_k^f)^2 \right]$; then the composite fermions form two $\nu = -1$ IQH states, and the interspecies correlation is captured by $\prod_j^{N_b} \prod_k^{N_f} (z_j^b - z_k^f)$. In the thermodynamic limit, the numbers of particles and fluxes must satisfy $N_b = M_f$ and $N_f = M_b + M_f$ to realize Ψ_{SPT} . In addition to the ground state, we can create four types of elementary excitations that carry integral charges [72].

Topological properties of Ψ_{SPT} are encoded compactly in the Abelian Chern-Simons (CS) theory. The Lagrangian density is

$$\mathcal{L}_{\text{CS}} = \frac{1}{4\pi} K_{IJ} a_I da_J + \frac{t_I}{2\pi} A da_I, \quad (2)$$

where K is an integer-valued symmetric matrix, the a_I 's

are emergent gauge fields, and $a_I da_J \equiv \epsilon^{\mu\nu\lambda} a_{I,\mu} \partial_\nu a_{J,\lambda}$. Here we also include the coupling with a background $U(1)$ gauge field A , with integers t_I known as the charge vector. This formalism was originally proposed for intrinsic topological orders [73] but has also been very useful in studying SPT states [74]. The number of degenerate ground states on a torus is given by $|\det K|$. For the case with a unique ground state ($|\det K| = 1$), one can further show that there exist no topologically nontrivial excitations.

Inspired by the wave function Ψ_{SPT} , we consider the following K matrix and charge vector:

$$K_{\text{SPT}} = \begin{pmatrix} 0 & 1 \\ 1 & 1 \end{pmatrix}, \quad \mathbf{t}_{\text{SPT}} = \begin{pmatrix} e_b \\ e_f \end{pmatrix}. \quad (3)$$

Because K_{SPT} has determinant -1 and zero signature (hence no chiral central charge), the theory indeed describes a SPT state. The Hall conductance of the system is $\sigma_{xy} = \mathbf{t}_{\text{SPT}}^T K_{\text{SPT}}^{-1} \mathbf{t}_{\text{SPT}} = e_b(2e_f - e_b)$. If the system has an edge, there are two counterpropagating gapless modes with opposite chiralities, which can be protected by a $U(1)$ symmetry when $\sigma_{xy} \neq 0$ ($e_b \neq 0, 2e_f$). For the microscopic model studied below, the numbers of bosons and fermions are separately conserved, so we have a $U(1)_b \times U(1)_f$ symmetry. In this case, we can introduce two background gauge fields A_b and A_f that couple with the particles via

$$\mathbf{t}_{\text{SPT}}^b = \begin{pmatrix} e_b \\ 0 \end{pmatrix}, \quad \mathbf{t}_{\text{SPT}}^f = \begin{pmatrix} 0 \\ e_f \end{pmatrix}. \quad (4)$$

One can measure intraspecies Hall conductance (the response of one species to its associated field A_σ) and interspecies Hall conductance [the response of bosons to A_f or fermions to A_b]. The results can be organized as a matrix

$$\begin{pmatrix} \sigma_b & \sigma_{\text{mix}} \\ \sigma_{\text{mix}} & \sigma_f \end{pmatrix} = \begin{pmatrix} -e_b^2 & e_b e_f \\ e_b e_f & 0 \end{pmatrix}. \quad (5)$$

In other words, the response theory contains a bosonic CS term $-\frac{1}{4\pi} e_b^2 A_b dA_b$ and a mutual CS term $\frac{1}{2\pi} e_b e_f A_b dA_f$.

Now we turn to the FQH state in which the bosons and fermions are decoupled but still have suitable intraspecies interactions. At individual filling factors $\nu_b = 1/2$ and $\nu_f = 2/3$, the system is described by

$$\Psi_{\text{FQH}} \sim \Phi_1(\{z_j^b\}) \Phi_2^*(\{z_j^f\}) \times \prod_{j < k}^{N_b} (z_j^b - z_k^b) \prod_{j < k}^{N_f} (z_j^f - z_k^f)^2. \quad (6)$$

Intuitively, the particles are also converted to composites by the Jastrow factors, which now form their respective IQH states with $\nu = 1$ (bosons) and -2 (fermions). In the CS theory, the bosonic FQH state has

$K_b = 2$ and $\mathbf{t}_{\text{FQH}}^b = e_b$ and the fermionic FQH state has

$$K_f = \begin{pmatrix} 1 & 0 \\ 0 & -3 \end{pmatrix}, \quad \mathbf{t}_{\text{FQH}}^f = e_f \begin{pmatrix} 1 \\ 1 \end{pmatrix}. \quad (7)$$

Quantum phase transitions — If we turn on inter-species interaction, it is possible to induce a quantum phase transition from the FQH state to the SPT state. To gain some intuition about how the transition takes place, we may strip off the flux attachment factors in Ψ_{SPT} and Ψ_{FQH} to consider a transition between the states $\Phi_1(\{z_j^b\})\Phi_2^*(\{z_j^f\})$ and $\Phi_1^*(\{z_j^b\})\Phi_1(\{z_j^f\})\prod_j^{N_b}\prod_k^{N_f}(z_j^b - z_k^f)$. The latter state is actually a superfluid because its K matrix

$$\begin{pmatrix} -1 & 1 \\ 1 & -1 \end{pmatrix} \quad (8)$$

has zero determinant. This is reminiscent of the well-known exciton condensate in quantum Hall bilayers [75], but there the K matrix has 1 on the diagonal. In short, the transition may be understood as composite fermions change from two decoupled IQH states to one correlated superfluid.

This intuitive picture can be formalized using a field theory. It is helpful to perform a $\text{GL}(2, \mathbb{Z})$ transformation such that the K matrix and charge vector for the fermionic state become

$$K_f = \begin{pmatrix} 1 & 1 \\ 1 & -2 \end{pmatrix}, \quad \mathbf{t}_{\text{FQH}}^f = e_f \begin{pmatrix} 1 \\ 0 \end{pmatrix}. \quad (9)$$

To combine the bosonic and fermionic FQH states, we rename the emergent gauge field for bosons as a_1 and the fields for fermions as a_2 and a_3 . The resulting CS theory has 3×3 -dimensional K matrix $K_{\text{FQH}} = K_b \oplus K_f$ and charge vector $\mathbf{t}_{\text{FQH}} = \mathbf{t}_{\text{FQH}}^b \oplus \mathbf{t}_{\text{FQH}}^f$. Inspired by the analysis based on wave functions, we proceed to consider what happens when a_1 and a_3 are locked together by a Higgs field. Specifically, a complex scalar ϕ is introduced to construct the Lagrangian density

$$\mathcal{L}_{\text{mix}} = \mathcal{L}_b + \mathcal{L}_f + |(\partial - ia_1 + ia_3)\phi|^2 + r|\phi|^2 + u|\phi|^4 + \dots \quad (10)$$

When $r > 0$, ϕ is gapped and can be integrated out to reproduce the CS theory for the FQH state. When $r < 0$, ϕ condenses to generate the Higgs phase in which a_3 can be eliminated by setting it to a_1 . This leads to

$$\frac{1}{2\pi}a_1 da_2 + \frac{1}{4\pi}a_2 da_2 + \frac{e_b}{2\pi}A_b da_1 + \frac{e_f}{2\pi}A_f da_2, \quad (11)$$

which is exactly the same as \mathcal{L}_{SPT} . For a whole family of systems with filling factors $\nu_b = p/(p+1)$ and $\nu_f = (p+1)/(2p+1)$, we have uncovered similar mechanisms for continuous phase transitions and constructed the associated field theories [72].

To further understand the critical theory, we perform the following $\text{GL}(3, \mathbb{Z})$ basis transformation for the gauge fields:

$$\begin{pmatrix} a_1 \\ a_2 \\ a_3 \end{pmatrix} = \begin{pmatrix} 3 & 1 & -1 \\ -2 & 0 & 1 \\ 2 & 1 & -1 \end{pmatrix} \begin{pmatrix} b_1 \\ b_2 \\ b_3 \end{pmatrix}. \quad (12)$$

The K matrix is

$$\begin{pmatrix} 6 & 0 & 0 \\ 0 & 0 & 1 \\ 0 & 1 & -1 \end{pmatrix} \quad (13)$$

in the new basis. The critical theory becomes

$$\frac{6}{4\pi}b_1 db_1 + |(\partial - ib_1)\phi|^2 + r|\phi|^2 + u|\phi|^4 + \dots, \quad (14)$$

so $a_1 - a_3 = b_1$ couples to ϕ while b_2 and b_3 decouple from critical fluctuations. Interestingly, this theory also describes a continuous transition between a $1/6$ Laughlin state and a trivial insulator. It is a strongly coupled theory for which analytical results are available only in the limit with a large number of boson flavors and a large CS level. In this case, (the generalization of) Eq. (14) indeed flows to a conformal fixed point at low energy. It is thus quite reasonable to conjecture that Eq. (14) describes an unconventional quantum critical point. For the transitions at other filling factors, similar basis transformations can also be found [72].

Numerical results — It is not *a priori* clear that the SPT state can be realized using a simple microscopic Hamiltonian. To this end, we consider the many-body Hamiltonian for the bosons and fermions

$$H_{\text{mix}} = \sum_{j < k} 4\pi\ell_b^2 \delta(\mathbf{r}_j^b - \mathbf{r}_k^b) + \sum_{j < k} 4\pi\ell_f^4 \nabla^2 \delta(\mathbf{r}_j^f - \mathbf{r}_k^f) + g_m \sum_{j,k} 4\pi\ell_b\ell_f \delta(\mathbf{r}_j^b - \mathbf{r}_k^f), \quad (15)$$

where ℓ_b (ℓ_f) is the magnetic length for bosons (fermions). It is necessary to introduce two magnetic lengths because the magnetic fluxes for the two types of particles are different. The unit of length is chosen to be ℓ_b . The particles are confined to their respective lowest Landau levels and higher levels are neglected. The first (second) term in H_{mix} corresponds to the zeroth (first) Haldane pseudopotential [76], so we know for sure that Ψ_{FQH} can be realized at $g_m = 0$. Exact diagonalizations of H_{mix} are performed on the torus [77] at many different $g_m \in [0, 1]$. The energy spectra are presented in Fig. 2 (a). A unique ground state is observed when $g_m \sim 1$, but there are six quasidegenerate ground states when $g_m \sim 0$ [78, 79]. This suggests that the Hamiltonian with $g_m \sim 1$ resides in the SPT phase. To further corroborate this claim, we have computed the Hall conductance matrix for several cases using the twisted boundary condition method [80, 81]. For simplicity, we choose

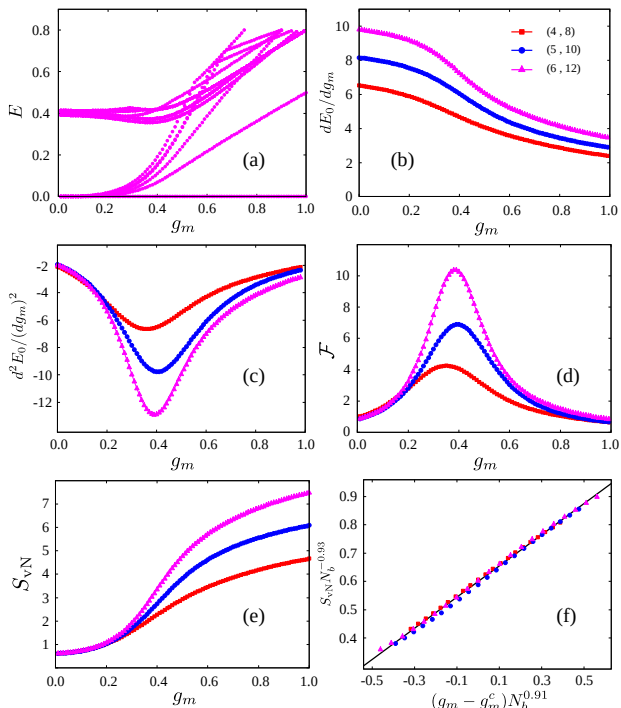


FIG. 2. Numerical results on the torus. (a) The low-lying energy levels of the $N_b = 6, N_f = 12$ system versus g_m . (b) The first-order derivative of the ground state energy. (c) The second-order derivative of the ground state energy. (d) The ground state fidelity susceptibility. (e) The von Neumann entanglement entropy between bosons and fermions. (f) The same data in (e) replotted to achieve data collapse. The numbers of particles (N_b, N_f) for panels (b)-(f) are indicated using the legend of (b).

$e_b = e_f = 1$ in Eq. (5) such that the intraspecies Hall conductances are -1 and 0 whereas the drag Hall conductance is 1 . The actual numbers obtained in numerical calculations are very close to these values (the deviation is smaller than 10^{-9}) [72].

The transition is inspected more closely using the lowest eigenvalue $E_0(g_m)$ and the associated eigenstate $|\Psi_0(g_m)\rangle$. The transition appears to be continuous, as one can see from the first-order derivative dE_0/dg_m in Fig. 2 (b). The transition point is found to be $g_m^c \approx 0.39$, where peaks appear in the second-order derivative d^2E_0/dg_m^2 as shown in Fig. 2 (c). The evolution of $|\Psi_0(g_m)\rangle$ can be characterized using the ground state fidelity susceptibility [82, 83]

$$\mathcal{F}(g_m) = \frac{2}{(\delta g_m)^2} \left[1 - |\langle \Psi_0(g_m) | \Psi_0(g_m + \delta g_m) \rangle| \right]. \quad (16)$$

As the system passes the transition point, the state changes abruptly such that \mathcal{F} attains a very large value. This picture is confirmed by the appearance of peaks around $g_m^c \approx 0.39$ in Fig. 2 (d). The continuous nature of this transition is further corroborated by density matrix renormalization group calculations [72, 84–

86]. In the vicinity of a critical point, critical scaling of physical quantities plays a prominent role. For symmetry-breaking phase transitions, correlation functions of local observables are routinely studied. However, they are not expected to give clear signatures due to the limited spatial extent of our system. To this end, we consider the quantum entanglement between the bosons and fermions. The reduced density matrix for the bosons is obtained by tracing out the fermions as $\rho_b = \text{Tr}_f |\Psi_0(g_m)\rangle \langle \Psi_0(g_m)|$. The von Neumann entanglement entropy $S_{vN} = -\text{Tr} \rho_b \ln \rho_b$ is presented in Fig. 2 (e). The boson-fermion entanglement is weak for small g_m but seems to obey the volume law in the SPT state. Unfortunately, we are not able to derive the scaling form of S_{vN} using field theory. We make a bold conjecture that $S_{vN}(g_m) N_b^\alpha = f[(g_m - g_m^c) N_b^\beta]$. The data points for $g_m \in [0.30, 0.50]$ can be collapsed on a straight line using $\alpha \approx -0.93$ and $\beta \approx 0.91$ as shown in Fig. 2 (f).

It is also helpful to employ the spherical geometry [76]. A great advantage is that Ψ_{SPT} (and the trial wave functions for excitations) can be constructed more easily [87, 88]. However, its curvature results in a shift quantum number and the filling factor in finite-size systems may not be equal to its thermodynamic value [89]. The system parameters should satisfy $M_b = 2(N_b - 1)$ for the bosonic $1/2$ state, $M_f = 3N_f/2$ for the fermionic $2/3$ state, and $M_b = N_f, M_f = N_b + N_f$ for the SPT state. This imposes the condition $N_b = N_f/2 + 1$ instead of $N_b = N_f/2$. For the $N_b = 5, N_f = 8$ system, Fig. 3 (a) displays the low-energy states of H_{mix} at $g_m = 1.0$ (plotted versus the total angular momentum L), which are compared with appropriate trial wave functions [72]. The overlap for the ground state is excellent (0.99), and those for the excitations are quite good (except for one state). To probe the edge physics, we turn to the real space entanglement spectrum [90–93]. For the $N_b = 7, N_f = 14$ system, the eigenvalues of the reduced density matrix for the southern hemisphere are shown in Fig. 3 (b). The good quantum numbers are the numbers of particles in the subspace and the z component of the angular momentum. As indicated in the figure, two edge modes with opposite chiralities can be identified. The counting $1, 1, 2, 3$ suggests that they are described by free bosons, which agrees with the CS theory.

Conclusions — In summary, we have proposed an SPT state in Bose-Fermi mixtures that could be realized using a simple Hamiltonian. By tuning the interspecies interaction, quantum phase transitions to FQH states with intrinsic topological order can be induced. The possibility that these transitions are continuous is revealed by critical field theory and substantiated by numerical results. We have also made a first attempt toward revealing critical scaling of the entanglement entropy. This is very premature due to the absence of reliable analytical results on the scaling function. Many questions remain to be answered. It will be interesting to further study criti-

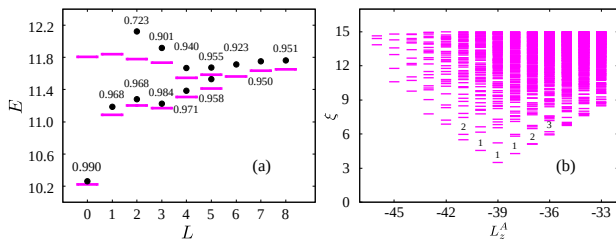


FIG. 3. Numerical results on the sphere. (a) The low-lying energy levels of the $N_b = 5$, $N_f = 8$ system. The lines (dots) represent exact eigenstates (trial wave functions) and the numbers are their overlaps. (b) The entanglement spectrum of the $N_b = 7$, $N_f = 12$ system in the sector for which the southern hemisphere has four bosons and six fermions.

cal properties of the theory in Eq. (14). More broadly, a general picture for the transitions between strongly correlated states in the quantum Hall regime is very desirable. The effects of disorder and other imperfections that could appear in realistic systems should also be investigated. On the experimental frontier, multiple groups have reported FQH states in moiré systems without external magnetic field [94–98]. A primitive idea is stacking these FQH states with the Laughlin state of excitons [68] to study phase transitions. Since Bose-Fermi mixtures have been realized in Refs. [66, 67] using electrons and excitons, it is natural to explore topological states in such systems.

Note added — While finalizing the manuscript, we noticed a preprint on the transition between a FQH state and an exciton condensate in quantum Hall bilayers [99]. The physics is quite different from the FQH-SPT transition studied in this work.

Acknowledgements — We thank Chao-Ming Jian, Zhao Liu, Xin Wan, and Hao Wang for helpful conversations. This work was supported by the NNSF of China under grant No. 12174130 (Y.-H. W.), the Deutsche Forschungsgemeinschaft through project A06 of SFB 1143 under project No. 247310070 (H.-H. T.), and NSF under award No. DMR-1846109 (M.C.).

[1] K. v. Klitzing, G. Dorda, and M. Pepper, *Phys. Rev. Lett.* **45**, 494 (1980).
 [2] D. C. Tsui, H. L. Stormer, and A. C. Gossard, *Phys. Rev. Lett.* **48**, 1559 (1982).
 [3] R. B. Laughlin, *Phys. Rev. Lett.* **50**, 1395 (1983).
 [4] J. T. Chalker and P. D. Coddington, *J. Phys. C: Solid State Phys.* **21**, 2665 (1988).
 [5] B. Huckestein and B. Kramer, *Phys. Rev. Lett.* **64**, 1437 (1990).
 [6] Y. Huo and R. N. Bhatt, *Phys. Rev. Lett.* **68**, 1375 (1992).
 [7] D.-H. Lee, Z. Wang, and S. Kivelson, *Phys. Rev. Lett.* **70**, 4130 (1993).

[8] J. K. Jain, S. A. Kivelson, and N. Trivedi, *Phys. Rev. Lett.* **64**, 1297 (1990).
 [9] S. Kivelson, D.-H. Lee, and S.-C. Zhang, *Phys. Rev. B* **46**, 2223 (1992).
 [10] W. Zhu, Z. Liu, F. D. M. Haldane, and D. N. Sheng, *Phys. Rev. B* **94**, 245147 (2016).
 [11] J. Y. Lee, C. Wang, M. P. Zaletel, A. Vishwanath, and Y.-C. He, *Phys. Rev. X* **8**, 031015 (2018).
 [12] X.-G. Wen and Y.-S. Wu, *Phys. Rev. Lett.* **70**, 1501 (1993).
 [13] J. Ye and S. Sachdev, *Phys. Rev. Lett.* **80**, 5409 (1998).
 [14] M. Barkeshli and J. McGreevy, *Phys. Rev. B* **89**, 235116 (2014).
 [15] M. Mulligan, C. Nayak, and S. Kachru, *Phys. Rev. B* **82**, 085102 (2010).
 [16] M. Barkeshli and X.-G. Wen, *Phys. Rev. B* **84**, 115121 (2011).
 [17] Z. Liu and R. N. Bhatt, *Phys. Rev. Lett.* **117**, 206801 (2016).
 [18] J. Motruk and F. Pollmann, *Phys. Rev. B* **96**, 165107 (2017).
 [19] W. Zhu and D. N. Sheng, *Phys. Rev. Lett.* **123**, 056804 (2019).
 [20] Z. Zhu, D. N. Sheng, and I. Sodemann, *Phys. Rev. Lett.* **124**, 097604 (2020).
 [21] T.-S. Zeng, *Phys. Rev. B* **103**, 085122 (2021).
 [22] P. Kumar and R. N. Bhatt, *Phys. Rev. B* **106**, 115101 (2022).
 [23] M. Z. Hasan and C. L. Kane, *Rev. Mod. Phys.* **82**, 3045 (2010).
 [24] X.-L. Qi and S.-C. Zhang, *Rev. Mod. Phys.* **83**, 1057 (2011).
 [25] C. L. Kane and E. J. Mele, *Phys. Rev. Lett.* **95**, 226801 (2005).
 [26] C. L. Kane and E. J. Mele, *Phys. Rev. Lett.* **95**, 146802 (2005).
 [27] B. A. Bernevig and S.-C. Zhang, *Phys. Rev. Lett.* **96**, 106802 (2006).
 [28] B. A. Bernevig, T. L. Hughes, and S.-C. Zhang, *Science* **314**, 1757 (2006).
 [29] A. P. Schnyder, S. Ryu, A. Furusaki, and A. W. W. Ludwig, *Phys. Rev. B* **78**, 195125 (2008).
 [30] A. Kitaev, *AIP Conf. Proc.* **1134**, 22 (2009).
 [31] Z.-C. Gu and X.-G. Wen, *Phys. Rev. B* **80**, 155131 (2009).
 [32] A. Kitaev, *KITP online talks* (2011).
 [33] X. Chen, Z.-C. Gu, Z.-X. Liu, and X.-G. Wen, *Science* **338**, 1604 (2012).
 [34] X. Chen, Z.-C. Gu, Z.-X. Liu, and X.-G. Wen, *Phys. Rev. B* **87**, 155114 (2013).
 [35] T. Senthil, *Ann. Rev. Cond. Matter Phys.* **6**, 299 (2015).
 [36] W. Son, L. Amico, R. Fazio, A. Hamma, S. Pascazio, and V. Vedral, *Europhys. Lett.* **95**, 50001 (2011).
 [37] T. Mizushima, M. Sato, and K. Machida, *Phys. Rev. Lett.* **109**, 165301 (2012).
 [38] T. Grover and A. Vishwanath, *Phys. Rev. B* **87**, 045129 (2013).
 [39] C. Xu and T. Senthil, *Phys. Rev. B* **87**, 174412 (2013).
 [40] Y.-M. Lu and D.-H. Lee, *Phys. Rev. B* **89**, 195143 (2014).
 [41] A. Kshetrimayum, H.-H. Tu, and R. Orús, *Phys. Rev. B* **91**, 205118 (2015).
 [42] T. Scaffidi and Z. Ringel, *Phys. Rev. B* **93**, 115105 (2016).
 [43] Y.-Z. You, Z. Bi, D. Mao, and C. Xu, *Phys. Rev. B* **93**, 125101 (2016).

- [44] H.-Q. Wu, Y.-Y. He, Y.-Z. You, T. Yoshida, N. Kawakami, C. Xu, Z. Y. Meng, and Z.-Y. Lu, *Phys. Rev. B* **94**, 165121 (2016).
- [45] L. Tsui, Y.-T. Huang, H.-C. Jiang, and D.-H. Lee, *Nucl. Phys. B* **919**, 470 (2017).
- [46] T. Scaffidi, D. E. Parker, and R. Vasseur, *Phys. Rev. X* **7**, 041048 (2017).
- [47] D. E. Parker, T. Scaffidi, and R. Vasseur, *Phys. Rev. B* **97**, 165114 (2018).
- [48] T.-S. Zeng, D. N. Sheng, and W. Zhu, *Phys. Rev. B* **101**, 035138 (2020).
- [49] Y. Xu, X.-C. Wu, C.-M. Jian, and C. Xu, *Phys. Rev. B* **101**, 184419 (2020).
- [50] C.-M. Jian, Y. Xu, X.-C. Wu, and C. Xu, *SciPost Phys.* **10**, 033 (2021).
- [51] M. Dupont, S. Gazit, and T. Scaffidi, *Phys. Rev. B* **103**, L140412 (2021).
- [52] M. Dupont, S. Gazit, and T. Scaffidi, *Phys. Rev. B* **103**, 144437 (2021).
- [53] N. Gemelke, E. Sarajlic, and S. Chu, [arXiv:1007.2677](https://arxiv.org/abs/1007.2677).
- [54] M. Aidelsburger, M. Atala, M. Lohse, J. T. Barreiro, B. Paredes, and I. Bloch, *Phys. Rev. Lett.* **111**, 185301 (2013).
- [55] M. E. Tai, A. Lukin, M. Rispoli, R. Schittko, T. Menke, D. Borgnia, P. M. Preiss, F. Grusdt, A. M. Kaufman, and M. Greiner, *Nature* **546**, 519 (2017).
- [56] L. W. Clark, N. Schine, C. Baum, N. Jia, and J. Simon, *Nature* **582**, 41 (2019).
- [57] R. J. Fletcher, A. Shaffer, C. C. Wilson, P. B. Patel, Z. Yan, V. Crépel, B. Mukherjee, and M. W. Zwierlein, *Science* **372**, 1318 (2021).
- [58] B. Mukherjee, A. Shaffer, P. B. Patel, Z. Yan, C. C. Wilson, V. Crépel, R. J. Fletcher, and M. Zwierlein, *Nature* **601**, 58 (2022).
- [59] J. Léonard, S. Kim, J. Kwan, P. Segura, F. Grusdt, C. Repellin, N. Goldman, and M. Greiner, *Nature* **619**, 495 (2023).
- [60] D.-W. Zhang, Y.-Q. Zhu, Y. X. Zhao, H. Yan, and S.-L. Zhu, *Adv. Phys.* **67**, 253 (2018).
- [61] N. R. Cooper, J. Dalibard, and I. B. Spielman, *Rev. Mod. Phys.* **91**, 015005 (2019).
- [62] A. G. Truscott, K. E. Strecker, W. I. McAlexander, G. B. Partridge, and R. G. Hulet, *Science* **291**, 2570 (2001).
- [63] G. Modugno, G. Roati, F. Riboli, F. Ferlaino, R. J. Brecha, and M. Inguscio, *Science* **297**, 2240 (2002).
- [64] I. Ferrier-Barbut, M. Delehaye, S. Laurent, A. T. Grier, M. Pierce, B. S. Rem, F. Chevy, and C. Salomon, *Science* **345**, 1035 (2014).
- [65] X.-C. Yao, H.-Z. Chen, Y.-P. Wu, X.-P. Liu, X.-Q. Wang, X. Jiang, Y. Deng, Y.-A. Chen, and J.-W. Pan, *Phys. Rev. Lett.* **117**, 145301 (2016).
- [66] B. Gao, D. G. Suárez-Forero, S. Sarkar, T.-S. Huang, D. Session, M. J. Mehrabad, R. Ni, M. Xie, J. Vannucci, S. Mittal, K. Watanabe, T. Taniguchi, A. Imamoglu, Y. Zhou, and M. Hafezi, [arXiv:2304.09731](https://arxiv.org/abs/2304.09731).
- [67] R. Qi, A. Y. Joe, Z. Zhang, Y. Zeng, T. Zheng, Q. Feng, E. Regan, J. Xie, Z. Lu, T. Taniguchi, K. Watanabe, S. Tongay, M. F. Crommie, A. H. MacDonald, and F. Wang, [arXiv:2306.13265](https://arxiv.org/abs/2306.13265).
- [68] R. Wang, T. A. Sedrakyan, B. Wang, L. Du, and R.-R. Du, *Nature* **619**, 57 (2023).
- [69] N. Stefanidis and I. Sodemann, *Phys. Rev. B* **102**, 035158 (2020).
- [70] Y. H. Kwan, Y. Hu, S. H. Simon, and S. A. Parameswaran, *Phys. Rev. B* **105**, 235121 (2022).
- [71] J. K. Jain, *Phys. Rev. Lett.* **63**, 199 (1989).
- [72] See the Supplemental Material for more analysis of the trial wave functions, other possible phase transitions, details about the Hall conductance matrix, and additional numerical results.
- [73] X. G. Wen and A. Zee, *Phys. Rev. B* **46**, 2290 (1992).
- [74] Y.-M. Lu and A. Vishwanath, *Phys. Rev. B* **86**, 125119 (2012).
- [75] J. P. Eisenstein, *Ann. Rev. Cond. Matter Phys.* **5**, 159 (2014).
- [76] F. D. M. Haldane, *Phys. Rev. Lett.* **51**, 605 (1983).
- [77] D. Yoshioka, B. I. Halperin, and P. A. Lee, *Phys. Rev. Lett.* **50**, 1219 (1983).
- [78] F. D. M. Haldane, *Phys. Rev. Lett.* **55**, 2095 (1985).
- [79] X. G. Wen and Q. Niu, *Phys. Rev. B* **41**, 9377 (1990).
- [80] Q. Niu, D. J. Thouless, and Y.-S. Wu, *Phys. Rev. B* **31**, 3372 (1985).
- [81] T. Fukui, Y. Hatsugai, and H. Suzuki, *J. Phys. Soc. Jpn* **74**, 1674 (2005).
- [82] M. Cozzini, R. Ionicioiu, and P. Zanardi, *Phys. Rev. B* **76**, 104420 (2007).
- [83] W.-L. You, Y.-W. Li, and S.-J. Gu, *Phys. Rev. E* **76**, 022101 (2007).
- [84] S. R. White, *Phys. Rev. Lett.* **69**, 2863 (1992).
- [85] U. Schollwöck, *Ann. Phys.* **326**, 96 (2011).
- [86] Z.-X. Hu, Z. Papić, S. Johri, R. N. Bhatt, and P. Schmitteckert, *Phys. Lett. A* **376**, 2157 (2012).
- [87] M. Hermanns, *Phys. Rev. B* **87**, 235128 (2013).
- [88] S. Pu, Y.-H. Wu, and J. K. Jain, *Phys. Rev. B* **96**, 195302 (2017).
- [89] X. G. Wen and A. Zee, *Phys. Rev. Lett.* **69**, 953 (1992).
- [90] H. Li and F. D. M. Haldane, *Phys. Rev. Lett.* **101**, 010504 (2008).
- [91] J. Dubail, N. Read, and E. H. Rezayi, *Phys. Rev. B* **85**, 115321 (2012).
- [92] A. Sterdyniak, A. Chandran, N. Regnault, B. A. Bernevig, and P. Bonderson, *Phys. Rev. B* **85**, 125308 (2012).
- [93] I. D. Rodríguez, S. H. Simon, and J. K. Slingerland, *Phys. Rev. Lett.* **108**, 256806 (2012).
- [94] J. Cai, E. Anderson, C. Wang, X. Zhang, X. Liu, W. Holtzmann, Y. Zhang, F. Fan, T. Taniguchi, K. Watanabe, Y. Ran, T. Cao, L. Fu, D. Xiao, W. Yao, and X. Xu, *Nature* **622**, 63 (2023).
- [95] Y. Zeng, Z. Xia, K. Kang, J. Zhu, P. Knüppel, C. Vaswani, K. Watanabe, T. Taniguchi, K. F. Mak, and J. Shan, [arXiv:2305.00973](https://arxiv.org/abs/2305.00973).
- [96] H. Park, J. Cai, E. Anderson, Y. Zhang, J. Zhu, X. Liu, C. Wang, W. Holtzmann, C. Hu, Z. Liu, T. Taniguchi, K. Watanabe, J.-H. Chu, T. Cao, L. Fu, W. Yao, C.-Z. Chang, D. Cobden, D. Xiao, and X. Xu, *Nature* **622**, 74 (2023).
- [97] F. Xu, Z. Sun, T. Jia, C. Liu, C. Xu, C. Li, Y. Gu, K. Watanabe, T. Taniguchi, B. Tong, J. Jia, Z. Shi, S. Jiang, Y. Zhang, X. Liu, and T. Li, *Phys. Rev. X* **13**, 031037 (2023).
- [98] Z. Lu, T. Han, Y. Yao, A. P. Reddy, J. Yang, J. Seo, K. Watanabe, T. Taniguchi, L. Fu, and L. Ju, [arXiv:2309.17436](https://arxiv.org/abs/2309.17436).
- [99] Y.-H. Zhang, Z. Zhu, and A. Vishwanath, *Phys. Rev. X* **13**, 031023 (2023).

Appendix A: Elementary excitations of the SPT state

This section analyzes the elementary excitations of the symmetry-protected topological (SPT) state. Each boson (fermion) is attached with one (two) flux due to the same types of particles to become composite fermion. The interspecies correlation is accounted for by the Jastrow factor $\prod_{j < k} (z_j^b - z_k^f)$. Alternatively, this factor may be interpreted as performing interspecies flux attachment such that each boson (fermion) is attached with one flux due to the other types of particles. The composite fermions reside in effective fluxes M_b^* and M_f^* and form their respective effective Landau levels (LLs). If the system parameters are chosen properly, the lowest LLs for the two types of composite fermions are completely filled to produce the $\nu = -1$ IQH states. This corresponds to the ground state of the physical system. If there are holes in the lowest effective LLs and/or particles in higher effective LLs, we would have excited states of the physical system.

We consider the elementary neutral and charged excitations shown in Fig. A1. The latter name is borrowed from fractional quantum Hall (FQH) states, but it turns out that some of them may not carry charge. For the neutral excitations, the numbers of particles and the numbers of fluxes are the same as for the ground state, but one composite fermion is promoted from the fully occupied lowest effective LLs to the originally empty second effective LLs. For the charged excitations, there is only one hole in the lowest effective LLs or one particle in the second effective LLs. More specifically, the parameters should be adjusted as follows:

- type I: N_b, M_b, M_f increase by one unit and N_f is unchanged.
- type II: N_b increases by one unit and N_f, M_b, M_f are unchanged.
- type III: N_b, M_b, M_f decrease by one unit and N_f is unchanged.
- type IV: N_b decreases by one unit and N_f, M_b, M_f are unchanged.

It is a little difficult to analyze their charges because the numbers of particles and fluxes are changed simultaneously. To solve this problem, we analyze the consequences of adding or removing one physical particle. If one boson is added, only one type II excitation is created, so we conclude that it has charge e_b . If one fermion is added, one type I and one type II excitations are created, so we conclude that type I excitation has charge $e_f - e_b$. Type III and type IV excitations are created if one particle is removed, and similar analysis shows that their charges are $e_b - e_f$ and $-e_b$, respectively.

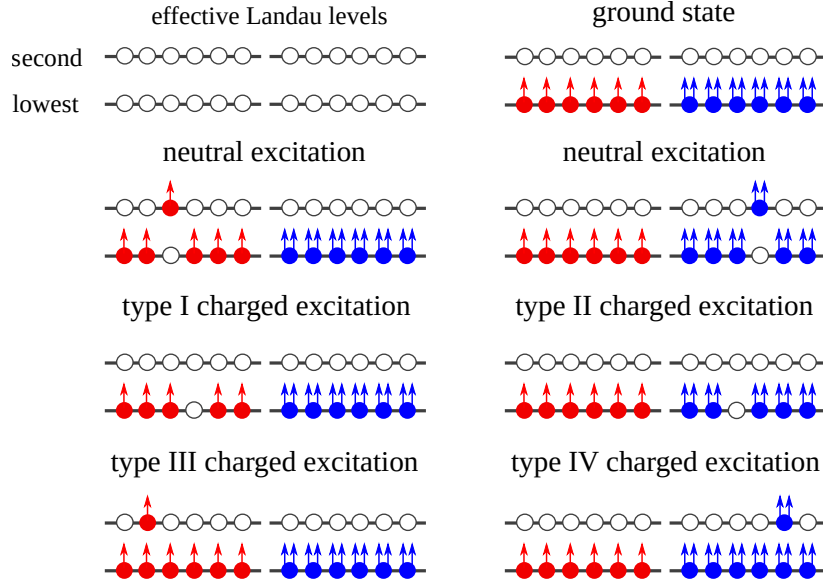


FIG. A1. Schematics of the elementary excitations of the SPT state.

Appendix B: Phase transitions between Jain's series and SPT states

This section generalizes the mechanism uncovered in the main text to a whole family of phase transitions between FQH and SPT states. On the FQH side, we have decoupled bosonic Jain state at $\nu_b = p/(p+1)$ and fermionic Jain state at $\nu_f = (p+1)/(2p+1)$ (with $p \in \mathbb{N}^+$). The SPT state is the same as in the main text, but the number of particles satisfy the constraint $N_b = pN_f/(p+1)$. The example studied in the main text corresponds to $p = 1$.

We briefly review the K matrix description of the FQH states in Jain's series. The bosonic Jain state at $\nu_b = p/(p+1)$ has K matrix

$$K_b = \begin{pmatrix} 1 & 1 & \cdots & 1 \\ 1 & 1 & \cdots & 1 \\ \vdots & \vdots & \ddots & \vdots \\ 1 & 1 & \cdots & 1 \end{pmatrix} + \mathbb{I}_{p \times p}. \quad (\text{A1})$$

and charge vector is $\mathbf{t}_{\text{FQH}}^b = e_b(1, 1, \dots, 1)^\top$. Here $\mathbb{I}_{p \times p}$ is the $p \times p$ dimensional identity matrix. In this state, composite fermions are obtained by attaching one flux to each boson, and they fill p Landau levels with Chern number 1. The fermionic FQH state at $\nu_f = (p+1)/(2p+1)$ has K matrix

$$K_f = 2 \begin{pmatrix} 1 & 1 & \cdots & 1 \\ 1 & 1 & \cdots & 1 \\ \vdots & \vdots & \ddots & \vdots \\ 1 & 1 & \cdots & 1 \end{pmatrix} - \mathbb{I}_{(p+1) \times (p+1)}. \quad (\text{A2})$$

and charge vector is $\mathbf{t}_{\text{FQH}}^f = e_f(1, 1, \dots, 1)^\top$. In this state, composite fermions are obtained by attaching two fluxes to each fermion, and they fill $p+1$ Landau levels with Chern number -1 .

When the two states are combined, the Chern-Simons theory would have $K_{\text{FQH}} = K_b \oplus K_f$ and $\mathbf{t}_{\text{FQH}} = \mathbf{t}_{\text{FQH}}^b \oplus \mathbf{t}_{\text{FQH}}^f$. An intuitive picture for the transition is that interspecies interaction induces strong correlation between composite fermions from the bosonic and fermionic Jain states. Formally, let us denote the gauge fields in the bosonic state as a_i ($i = 1, 2, \dots, p$) and those in the fermionic state as a_{p+j} ($j = 1, 2, \dots, p+1$). We propose that the transition is captured by the theory

$$\mathcal{L}_{\text{mix}} = \mathcal{L}_b + \mathcal{L}_f + |(\partial - ia_p + ia_{2p+1})\phi|^2 + r|\phi|^2 + u|\phi|^4 + \dots. \quad (\text{A3})$$

While no general proof has been found, it is very likely that the Higgsed phase is an invertible one and describes a SPT state. This claim can be verified easily for the $p = 2$ case. In the Higgsed phase, the K matrix takes the form

$$K_{\text{SPT}} = \begin{pmatrix} 2 & 0 & 0 & 1 \\ 0 & 1 & 2 & 2 \\ 0 & 2 & 1 & 2 \\ 1 & 2 & 2 & 3 \end{pmatrix} \quad (\text{A4})$$

and the charge vectors are $\mathbf{t}_{\text{SPT}}^b = e_b(1, 0, 0, 1)^\top$, $\mathbf{t}_{\text{SPT}}^f = e_f(0, 1, 1, 1)^\top$. K_{SPT} has unity determinant and zero signature. This state and the one studied in the main text have the same Hall responses. While these features suggest that they are in the same SPT phase, their K matrices do have different dimensions. To resolve this discrepancy, we change K_{SPT} using a $\text{GL}(4, \mathbb{Z})$ transformation:

$$\tilde{K}_{\text{SPT}} = W_{\text{SPT}}^\top K_{\text{SPT}} W_{\text{SPT}} = \begin{pmatrix} 0 & 1 & 0 & 0 \\ 1 & 0 & 0 & 0 \\ 0 & 0 & 0 & 1 \\ 0 & 0 & 1 & 1 \end{pmatrix}, \quad W_{\text{SPT}} = \begin{pmatrix} 1 & 1 & -1 & 1 \\ 0 & 1 & -1 & 1 \\ 1 & 0 & -1 & 1 \\ -1 & -1 & 2 & -1 \end{pmatrix}. \quad (\text{A5})$$

The charge vectors in the new basis are

$$\tilde{\mathbf{t}}_{\text{SPT}}^b = e_b(0, 0, 1, 0), \quad \tilde{\mathbf{t}}_{\text{SPT}}^f = e_f(0, 0, 0, 1). \quad (\text{A6})$$

The upper-left 2×2 block $\begin{pmatrix} 0 & 1 \\ 1 & 0 \end{pmatrix}$ is charge neutral and can be gapped out without breaking any symmetry. The lower-right 2×2 block and the associated components of the charge vectors are identical to those in the main text.

To better understand the critical theory, we can perform a $\text{GL}(5, \mathbb{Z})$ transformation to rewrite K_{FQH} as

$$\tilde{K}_{\text{FQH}} = W_2^T K_{\text{FQH}} W_2 = \begin{pmatrix} 15 & 0 & 0 & 0 & 0 \\ 0 & -9 & 5 & 1 & 13 \\ 0 & 5 & -1 & -1 & -4 \\ 0 & 1 & -1 & 0 & -2 \\ 0 & 13 & -4 & -2 & -14 \end{pmatrix}, \quad W_2 = \begin{pmatrix} -5 & -5 & 1 & 1 & 5 \\ 10 & 11 & -2 & -2 & -10 \\ -6 & -6 & 2 & 1 & 6 \\ -6 & -6 & 1 & 1 & 6 \\ 9 & 11 & -2 & -2 & -10 \end{pmatrix}. \quad (\text{A7})$$

The upper-left corner of \tilde{K}_{FQH} decouples from the lower-right 4×4 block that has unity determinant and zero signature. In the transformed theory, we have gauge fields b_j that are related to the a_j 's via $\mathbf{b} = W_2^{-1} \mathbf{a}$. The critical theory is simplified to

$$\mathcal{L} = \frac{15}{4\pi} b_1 db_1 + |(\partial - ib_1)\phi|^2 + r|\phi|^2 + u|\phi|^4 + \dots \quad (\text{A8})$$

with $b_1 = a_2 - a_5$. Numerical calculations have been performed for the $p = 2$ case and the results are presented in Fig. A2. It is plausible that the transition is continuous, but finite-size effect is quite strong here.

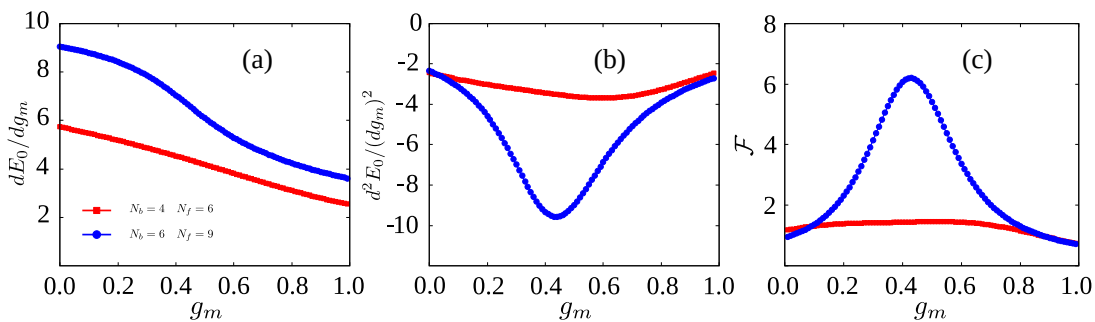


FIG. A2. Numerical results on the torus for the $p = 2$ case. (a) The first-order derivative of the ground state energy. (b) The second-order derivative of the ground state energy. (c) The ground state fidelity susceptibility.

Appendix C: Details about the Hall conductance matrix

This section explains in detail how to compute the Hall conductance matrix. The system is placed on a rectangular torus whose two sides have lengths L_x and L_y . The unit vectors along the two directions of the torus are denoted as \mathbf{e}_x and \mathbf{e}_y . The reciprocal vectors are

$$\mathbf{G}_1 = \frac{2\pi}{L_x} \mathbf{e}_x, \quad \mathbf{G}_2 = \frac{2\pi}{L_y} \mathbf{e}_y. \quad (\text{A9})$$

The translations along $L_x \mathbf{e}_x$ and $L_y \mathbf{e}_y$ must commute. The magnetic fluxes N_ϕ^σ for the two layers are constrained by the equation

$$2\pi \ell_\sigma^2 N_\phi^\sigma = L_x L_y. \quad (\text{A10})$$

The many-body Chern numbers are computed by applying twisted boundary conditions in the system [80]. For our bilayer system, there are four boundary twist angles θ_x^σ and θ_y^σ . In the presence of these angles, the single-particle eigenstates are

$$\begin{aligned} \phi_m^\sigma(x, y, \theta_x, \theta_y) &= \frac{1}{(\sqrt{\pi} \ell_\sigma L_y)^{1/2}} \sum_k^{\mathbb{Z}} \exp(ik\theta_x) \\ &\times \exp \left\{ -\frac{1}{2} \left[\frac{x}{\ell_B} - \frac{2\pi \ell_\sigma}{L_y} \left(\frac{\theta_y}{2\pi} + m + k N_\phi^\sigma \right) \right]^2 + i \frac{2\pi y}{L_y} \left(\frac{\theta_y}{2\pi} + m + k N_\phi^\sigma \right) \right\}. \end{aligned} \quad (\text{A11})$$

The creation (annihilation) operator associated with $\phi_m^\sigma(x, y, \theta_x, \theta_y)$ is denoted as $C_{\sigma, m}^\dagger$ ($C_{\sigma, m}$).

For a general two-body potential $V^{\sigma\tau}(\mathbf{r}_1 - \mathbf{r}_2)$, the second quantized form is

$$H = \frac{1}{2} \sum_{\sigma,\tau} \sum_{\{m_i\}} V_{m_1 m_2 m_3 m_4}^{\sigma\tau} C_{\sigma, m_1}^\dagger C_{\tau, m_2}^\dagger C_{\tau, m_4} C_{\sigma, m_3} \quad (\text{A12})$$

with

$$V_{m_1 m_2 m_3 m_4}^{\sigma\tau} = \int d\mathbf{r}_1 \int d\mathbf{r}_2 [\phi_{m_1}^\sigma(\mathbf{r}_1)]^* [\phi_{m_2}^\tau(\mathbf{r}_2)]^* V^{\sigma\tau}(\mathbf{r}_1 - \mathbf{r}_2) \phi_{m_4}^\tau(\mathbf{r}_2) \phi_{m_3}^\sigma(\mathbf{r}_1). \quad (\text{A13})$$

It is convenient to perform Fourier transform on $V^{\sigma\tau}(\mathbf{r}_1 - \mathbf{r}_2)$ such that the Hamiltonian becomes

$$H = \frac{1}{2L_x L_y} \sum_{\mathbf{q}} V^{\sigma\tau}(\mathbf{q}) : \rho^\sigma(\mathbf{q}) \rho^\tau(-\mathbf{q}) : \quad (\text{A14})$$

and

$$\begin{aligned} \rho^\sigma(\mathbf{q}) &= \int d\mathbf{r}_1 \sum_{m_1, m_3} [\phi_{m_1}^\sigma(\mathbf{r}_1)]^* \exp(i\mathbf{q} \cdot \mathbf{r}_1) \phi_{m_3}^\sigma(\mathbf{r}_1) C_{\sigma, m_1}^\dagger C_{\sigma, m_3}, \\ \rho^\tau(-\mathbf{q}) &= \int d\mathbf{r}_2 \sum_{m_2, m_4} [\phi_{m_2}^\tau(\mathbf{r}_2)]^* \exp(-i\mathbf{q} \cdot \mathbf{r}_2) \phi_{m_4}^\tau(\mathbf{r}_2) C_{\tau, m_2}^\dagger C_{\tau, m_4}. \end{aligned} \quad (\text{A15})$$

The integrals can be evaluated to yield

$$\begin{aligned} H &= \frac{1}{2L_x L_y} \sum_{\sigma,\tau} \sum_{\{m_i\}} \sum_{q_1, q_2} V(\mathbf{q}) \exp\left\{-\frac{1}{4}|\mathbf{q}|^2 (\ell_\sigma^2 + \ell_\tau^2)\right\} \\ &\times \exp\left[i\frac{\theta_x^\sigma}{N_\phi^\sigma}(m_1 - m_3 - q_2)\right] \exp\left[i\frac{\theta_x^\tau}{N_\phi^\tau}(m_2 - m_4 + q_2)\right] \\ &\times \exp\left[i\frac{\pi q_1}{N_\phi^\sigma}\left(\frac{\theta_y^\sigma}{\pi} + 2m_1 - q_2\right) - i\frac{\pi q_1}{N_\phi^\tau}\left(\frac{\theta_y^\tau}{\pi} + 2m_2 + q_2\right)\right] \\ &\times \tilde{\delta}_{m_1, m_3 + q_2} \tilde{\delta}_{m_2, m_4 - q_2} C_{\sigma, m_1}^\dagger C_{\tau, m_2}^\dagger C_{\tau, m_4} C_{\sigma, m_3} \end{aligned} \quad (\text{A16})$$

where we have introduced the generalized Kronecker symbol

$$\tilde{\delta}_{s, t + q_2} = 1 \quad \text{if and only if} \quad s \bmod N_\phi = (t + q_2) \bmod N_\phi. \quad (\text{A17})$$

For a given set of boundary twist angles, the SPT phase has a unique ground state that we denote as $|\Phi(\theta_x^b, \theta_y^b, \theta_x^f, \theta_y^f)\rangle$. We perform another unitary transformation to define the state

$$|\Psi(\theta_x^b, \theta_y^b, \theta_x^f, \theta_y^f)\rangle = \exp\left[-i \sum_{\sigma=b,f} \sum_{k=1}^N \left(\frac{x_k}{L_x} \theta_x^\sigma + \frac{y_k}{L_y} \theta_y^\sigma\right)\right] |\Phi(\theta_x^b, \theta_y^b, \theta_x^f, \theta_y^f)\rangle. \quad (\text{A18})$$

The exponential can be decomposed to be a products of exponentials for each particle. The elements of the Hall conductance matrix are the Chern numbers

$$C_{\sigma\tau} = \frac{1}{2\pi i} \int_0^{2\pi} d\theta_x^\sigma \int_0^{2\pi} d\theta_y^\tau \left[\left\langle \frac{\partial \Psi}{\partial \theta_x^\sigma} \middle| \frac{\partial \Psi}{\partial \theta_y^\tau} \right\rangle - \left\langle \frac{\partial \Psi}{\partial \theta_y^\tau} \middle| \frac{\partial \Psi}{\partial \theta_x^\sigma} \right\rangle \right]. \quad (\text{A19})$$

In our calculation, the Wilson loop method is employed since it is more accurate than direct numerical integration [81]. Let us explain the procedure in detail using C_{bb} . No boundary twist angles are applied to the fermions so they are dropped from the formulas to avoid clutter. The interval $[0, 2\pi]$ is divided into S segments such that each segment has length $\Delta\theta = 2\pi/S$. The many-body Hamiltonian with $\theta_x^b = i\Delta\theta$ and $\theta_y^b = j\Delta\theta$ is diagonalized to generate the state $|\Psi(i, j)\rangle$. The non-unitary exponential Berry connections are defined as

$$\mathcal{A}_x^{bb}(i, j) = \langle \Psi(i, j) | \Psi(i+1, j) \rangle, \quad \mathcal{A}_y^{bb}(i, j) = \langle \Psi(i, j) | \Psi(i, j+1) \rangle. \quad (\text{A20})$$

This leads to the unitary Berry connections

$$A_x^{bb}(i, j) = \frac{\mathcal{A}_x^{bb}(i, j)}{|\mathcal{A}_x^{bb}(i, j)|}, \quad A_y^{bb}(i, j) = \frac{\mathcal{A}_y^{bb}(i, j)}{|\mathcal{A}_y^{bb}(i, j)|}. \quad (\text{A21})$$

For the plaquette whose lower-left corner is located at i, j , its U(1) Wilson loop is defined as

$$W_{bb}(i, j) = A_x^{bb}(i, j)A_y^{bb}(i+1, j) [A_x^{bb}(i, j+1)]^* [A_y^{bb}(i, j)]^*. \quad (\text{A22})$$

The Chern number is

$$C_{bb} = \frac{1}{2\pi} \sum_{i,j=0}^{S-1} \Im \log [W_{bb}(i, j)], \quad (\text{A23})$$

where the imaginary part is restricted to the range $(-\pi, \pi]$. For the Chern number $C_{\sigma\tau}$, we only need to use nonzero θ_x^σ and θ_y^τ and the procedure is similar.

The essential step in this method is computing the overlaps in Eq. (A20). It is important to recognize that the Fock states depend on the boundary twist angles, and we need to know the overlaps between the single-particle eigenstates with different angles. The unitary transformation in Eq. (A18) can be implemented by changing the single-particle eigenstates to

$$\begin{aligned} \tilde{\phi}_m^\sigma(x, y, \theta_x^\sigma, \theta_y^\sigma) &= \exp\left(-i\frac{\theta_x^\sigma x}{L_x} - i\frac{\theta_y^\sigma y}{L_y}\right) \frac{1}{(\sqrt{\pi}\ell_\sigma L_y)^{1/2}} \sum_k^{\mathbb{Z}} \exp(ik\theta_x^\sigma) \\ &\quad \times \exp\left\{-\frac{1}{2}\left[\frac{x}{\ell_\sigma} - \frac{2\pi\ell_\sigma}{L_y}\left(\frac{\theta_y^\sigma}{2\pi} + m + kN_\phi^\sigma\right)\right]^2 + i\frac{2\pi y}{L_y}\left(\frac{\theta_y^\sigma}{2\pi} + m + kN_\phi^\sigma\right)\right\} \\ &= \exp\left(-i\frac{\theta_x^\sigma x}{L_x}\right) \frac{1}{(\sqrt{\pi}\ell_B L_y)^{1/2}} \sum_k^{\mathbb{Z}} \exp(ik\theta_x^\sigma) \\ &\quad \times \exp\left\{-\frac{1}{2}\left[\frac{x}{\ell_\sigma} - \frac{2\pi\ell_\sigma}{L_y}\left(\frac{\theta_y^\sigma}{2\pi} + m + kN_\phi^\sigma\right)\right]^2 + i\frac{2\pi y}{L_y}(m + kN_\phi^\sigma)\right\} \end{aligned} \quad (\text{A24})$$

For two states with the same θ_x^σ , we have

$$\int d\mathbf{r} \left[\tilde{\phi}_{m_1}^\sigma(x, y, \theta_x^\sigma, \theta_y^\sigma)\right]^* \tilde{\phi}_{m_2}^\sigma(x, y, \theta_x^\sigma, \zeta_y^\sigma) = \delta_{m_1, m_2} \exp\left[-\frac{\ell_\sigma^2}{4L_y^2}(\zeta_y^\sigma - \theta_y^\sigma)^2\right]. \quad (\text{A25})$$

For two states with the same θ_y^σ , we have

$$\int d\mathbf{r} \left[\tilde{\phi}_{m_1}^\sigma(x, y, \theta_x^\sigma, \theta_y^\sigma)\right]^* \tilde{\phi}_{m_2}^\sigma(x, y, \zeta_x^\sigma, \theta_y^\sigma) = \delta_{m_1, m_2} \exp\left[-\frac{\ell_\sigma^2}{4L_x^2}(\zeta_x^\sigma - \theta_x^\sigma)^2 - \frac{i}{N_\phi^\sigma}\left(\frac{\theta_y^\sigma}{2\pi} + m_1\right)(\zeta_x^\sigma - \theta_x^\sigma)\right]. \quad (\text{A26})$$

In our calculations, the interval $[0, 2\pi]$ is divided into 20 segments. The Hall conductance matrix has been computed in many cases. For the SPT phase, only the absolute ground state is needed for this calculation. The matrix at $g_m = 1.0$ is

$$\begin{pmatrix} -1 & 1 \\ 1 & 0 \end{pmatrix} + \begin{pmatrix} 1.96 \times 10^{-10} & 3.79 \times 10^{-11} \\ 2.44 \times 10^{-10} & 3.07 \times 10^{-10} \end{pmatrix} \quad (\text{A27})$$

for $N_b = 4, N_f = 8$ and

$$\begin{pmatrix} -1 & 1 \\ 1 & 0 \end{pmatrix} + \begin{pmatrix} -4.06 \times 10^{-10} & 3.08 \times 10^{-10} \\ 6.43 \times 10^{-11} & -1.72 \times 10^{-10} \end{pmatrix} \quad (\text{A28})$$

for $N_b = 5, N_f = 10$. These agree with Eq. (5) in the main text. For the FQH phase, all six quasi-degenerate ground states should be included. The drag Hall conductance at $g_m = 0.2$ is -6.01×10^{-10} for $N_b = 4, N_f = 8$ and -2.56×10^{-9} for $N_b = 5, N_f = 10$. This confirms that the two species are independent.

Appendix D: Additional numerical results

The system size that can be accessed in exact diagonalization is limited by the exponential growth of the Hilbert space dimension. In many cases, it is possible to study larger systems using the density matrix renormalization group (DMRG), which searches for the ground state in the manifold of matrix product states [84, 85]. DMRG calculations have been performed using the Hamiltonian H_{mix} on the torus, but the results are not particularly successful. For the $N_b = 7, N_f = 14$ system, the first-order and second-order derivatives of the ground state energy $E_0(g_m)$ are presented in Fig. A3. The former curve is quite smooth but the latter curve has strong fluctuations. The first-order derivative is approximated by the difference

$$\frac{E_0(g_m + \delta g_m) - E_0(g_m)}{\delta g_m}. \quad (\text{A29})$$

To obtain accurate values with $\delta g_m = 0.01$, the uncertainty of E_0 should be less than $O(10^{-3})$, which is somewhat challenging but can be done in a reasonable amount of time. For the second-order derivative, accurate values can be obtained only if the uncertainty of E_0 is less than $O(10^{-5})$, which is too demanding and not achieved in our calculations. This is not surprising in view of the fundamental difficulty on the torus [86].

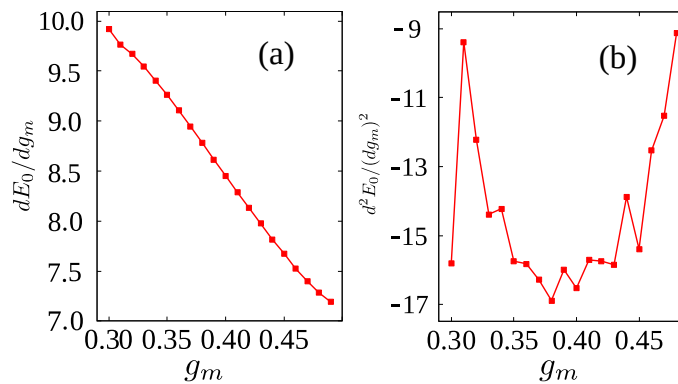


FIG. A3. DMRG results for the $N_b = 7, N_f = 14$ system on the torus. (a) The first-order derivative of the ground state energy. (b) The second-order derivative of the ground state energy.